Prog. Oceanog. Vol. 16, pp. 91–112, 1986.
Printed in Great Britain.

0079–6611/86 $0.00 + .50

A Synthesis of the First GARP Global Experiment (FGGE) in the Equatorial Atlantic Ocean

R. L. MOLINARI,* S. L. GARZOLI, E. J. KATZ,† D. E. HARRISON,‡ P. L. RICHARDSON,§ and G. REVERDIN‖

*National Oceanic and Atmospheric Administration, Atlantic Oceanographic and Meteorological Laboratory, Miami, Florida 33149, U.S.A.

†Lamont-Doherty Geological Observatory, Columbia University, Palisades, New York, U.S.A.

‡Massachusetts Institute of Technology Cambridge, Massachusetts, and National Oceanic and Atmospheric Administration, Pacific Marine Environmental Laboratory, Seattle, Washington, U.S.A.

§Woods Hole Oceanographic Institution, Woods Hole, Massachusetts 02543, U.S.A.

‖National Museum of Natural History, Physical Oceanography Laboratory, Paris, France

(*Submitted* 25 *February* 1985; *Received in final form* 4 *October* 1985)

Abstract—A synthesis of near-surface oceanographic and surface meteorological data collected during the First GARP Global Experiment, FGGE, is presented to portray the oceanic response to the seasonal wind forcing for the period December 1978 to November 1979, inclusive. Major wind events during FGGE are in phase with events given in climatology. In particular, the February–March–April relaxation and May enhancement of equatorial winds occurs within one month of the mean event. Accordingly, the oceanic responses, such as the May, June, July appearance of an equatorial cold water tongue, the acceleration of the South Equatorial Current (SEC) and the vertical displacement of the equatorial thermocline occur at the average time. Furthermore, the curl distribution in the vicinity of the North Equatorial Countercurrent (NECC) during 1979 is similar to the climatological distribution in terms of phase and amplitude, except for a westward displacement in the position of the maximum curl. As predicted from linear theory, the 1979 thermocline response across the NECC is in phase with the climatological response with a westward displacement of the maximum thermocline movement. Deeper than average equatorial thermoclines and a weaker SEC may, in part, be responsible for the anomalously warm sea-surface temperatures observed on the equator between 10°W and 30°W from June to November.

CONTENTS

1. Introduction 91
2. Data and Analysis 92
3. Atmospheric Observations 95
   3.1. Surface winds 95
   3.2. Surface heat fluxes 99
4. Oceanographic Observations 99
   4.1. Near surface currents 99
   4.2. Thermocline depth 104
   4.3. Sea-surface temperature 107
5. Discussion 108
Acknowledgements 111
References 111

1. INTRODUCTION

THE PURPOSE of the present paper is to synthesize the large set of oceanographic and surface meteorological data collected in the tropical Atlantic Ocean during 1979 within the context

of the First GARP Global Experiment (FGGE) in order to compose a picture of the annual cycle of near surface oceanic and meteorological features. The climatology of sea level meteorological variables and the upper ocean temperature and current fields of the tropical Atlantic Ocean have been reasonably well established in recent years (HASTENRATH and LAMB, 1977; MERLE, 1978; and RICHARDSON and MCKEE, 1984, for instance). However, generating climatologies is essentially a smoothing process. If our goal is to understand and model the response of the tropical ocean, climatology can be expected to describe reasonably well a mean state, but the smoothing is likely to mask phase relations between various processes. However, the existing climatology greatly enhances any attempt to understand a synoptic data set such as that collected during 1979. It can be used in two ways. If synoptic data are available, the climatology can be used to establish the "normalcy" of the particular year being studied. If no or few synoptic data are available, the climatology can be used to fill in data void areas. In this vein, we ask what was happening in the tropical Atlantic in 1979 as described by synoptic/climatological observations. In doing so, we rely heavily on previous studies based on FGGE data as reported on at a workshop convened in Venice, Italy (MCCREARY, MOORE and WITTE, 1981) and in the literature (see Table 1 for a partial list of FGGE publications).

2. DATA AND ANALYSES

We consider the tropical Atlantic Ocean bounded by the continents, 9°S and 9°N, during the FGGE year extending from December 1978 to November 1979. As we assume that the surface layers of the oceans are driven primarily by momentum and heat fluxes through the sea surface, we require descriptions of the surface meteorological fields which determine these fluxes. MOLINARI, FESTA and MARMOLEJO (1985a) used surface meteorological data

TABLE 1. PARTIAL LIST OF ARTICLES BASED ON DATA COLLECTED DURING FGGE

(A) *Observed Atmospheric Forcing*

Surface Wind Field	Surface Heat Fluxes
GARZOLI *et al.* (1982) SPETH and PANITZ (1983) MOLINARI *et al.* (1985a)	MOLINARI *et al.* (1985a)

(B) *Observed Oceanic Response*

Currents	Pressure Field/ Thermocline Depth	Temperature
KATZ *et al.* (1981) MOLINARI *et al.* (1981) MOLINARI (1982) MOLINARI (1983)	KATZ (1981) LASS *et al.* (1983) REVERDIN *et al.* (1985)	FAHRBACH (1983) FAHRBACH and BAUERFIEND (1982) MOLINARI *et al.* (1983, 1985a, b)

(C) *Modeled Oceanic Response*

KATZ and GARZOLI (1981)

obtained by merchant and research vessels during FGGE (Fig. 1) to generate mean monthly fields of surface wind, air temperature, cloud cover, sea surface temperature and specific humidity on a 2° × 2° grid. They computed standard error of the mean values for each 2° × 2° quadrangle. These errors include instrumental and geophysical noise. They then determined ensemble average error estimates for two classes of quadrangles, those within the shipping lanes and those outside the lanes. These errors are listed in Table 2. As expected, errors are considerably larger in the quadrangles outside the shipping lanes.

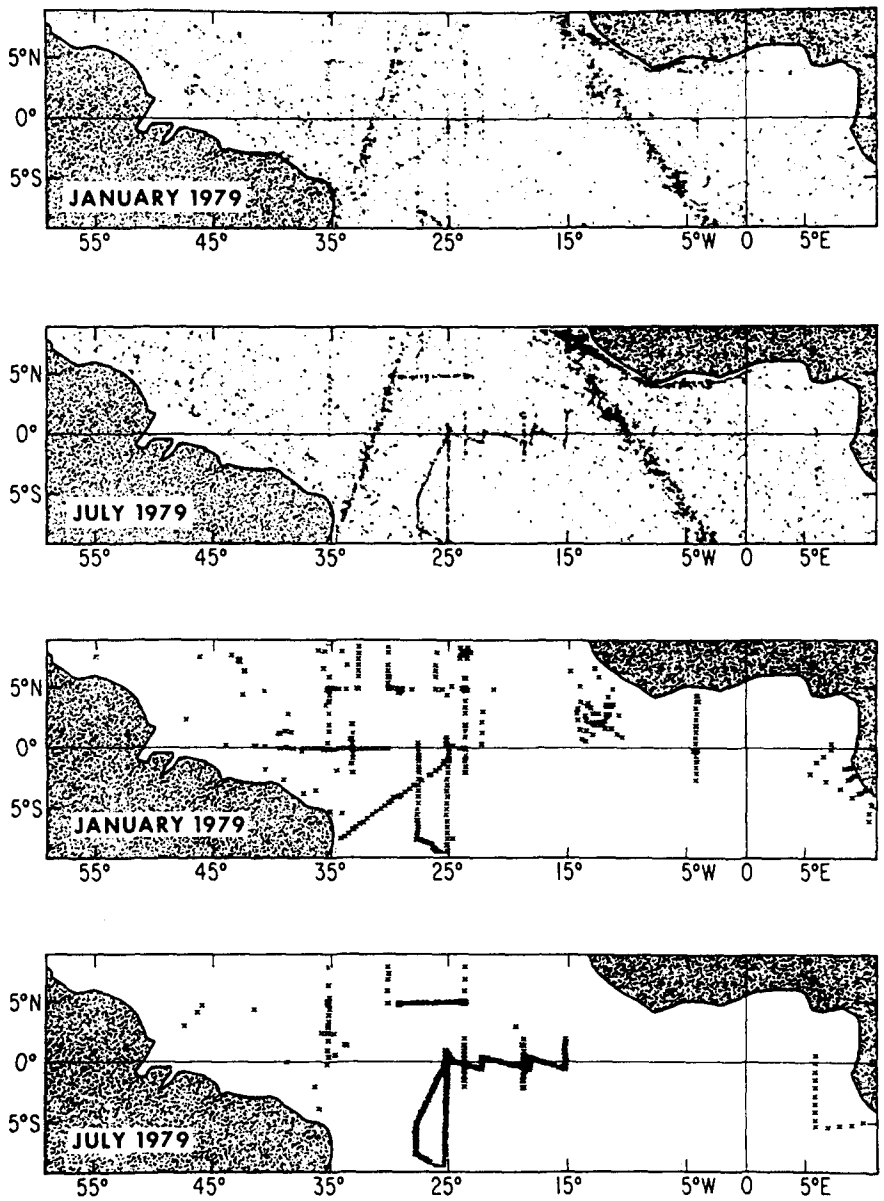

FIG. 1. Distributions of surface and subsurface oceanographic and surface meteorogical observations during two representative 1979 months.

TABLE 2. ENSEMBLE AVERAGE STANDARD ERROR OF THE MEAN VALUES FOR QUADRANGLES WITHIN THE SHIPPING LANES (> 15 VALUES) AND OUTSIDE THE SHIPPING LANES (< 10 VALUES), FROM MOLINARI *et al.* (1985a)

	> 15 Values	< 10 Values
SST (°C)	0.16	0.31
East wind component ($m\,sec^{-1}$)	0.36	0.66
North wind component ($m\,sec^{-1}$)	0.38	0.73
Air temperature (°C)	0.22	0.42
Cloud cover (tenths)	0.4	0.8
Dew point temperature (°C)	0.23	0.39

MOLINARI, FESTA and MARMOLEJO (1985a) used the surface meteorological data and the bulk aerodynamic formulas to compute surface latent and sensible heat fluxes, and net short and longwave radiation balances and the net oceanic heat gain (the sum of these fluxes). Using the uncertainty estimates listed in Table 2 and a propagation of error analysis (MEYER, 1975), they also computed error estimates for individual fluxes (as well as for specific humidity which is also computed from the variables given in Table 2). They noted that these errors are independent of any inadequacies in the bulk formulae and depend only on sampling and instrumental uncertainties. Their estimates are given in Table 3. These error estimates translate to errors in oceanic heat gain of the order of $40\,W\,m^{-2}$ within the shipping lanes and $60\,W\,m^{-2}$ outside. However, their comparisons of computed heat gains with observed changes in mixed layer temperature indicate that actual heat gain errors are probably less, of the order 20 to $30\,W\,m^{-2}$. Wind stress values are computed from the monthly mean wind components using a quadratic stress formulation and a constant drag coefficient of 1.4×10^{-3}, an average value for typical atmospheric conditions in the region (BUNKER, 1976).

We will describe the response of the near surface current and temperature fields. Surface currents are determined from ship-drift reports as described in MOLINARI, FESTA and MARMOLEJO (1985b). In addition to random errors of about $0.1\,m\,sec^{-1}$, they also show a systematic error (based on a comparison of the few available direct current observations and the ship drift data) in these observations of about $0.1\,m\,sec^{-1}$ to the west. The latter error is caused by windage effects on the ships. Direct observations of current collected during FGGE are also considered.

Subsurface temperature data availabe from an international fleet of research vessels (MOLINARI, KATZ, FAHRBACH, LASS and VOITURIEZ, 1983) are used to determine the

TABLE 3. ENSEMBLE AVERAGE STANDARD ERROR OF THE MEAN VALUES FOR QUADRANGLES WITHIN THE SHIPPING LANES (10 TO 15 VALUES) AND OUTSIDE THE SHIPPING LANES (5 TO 10 VALUES)

	10–15 Values	5–10 Values
Saturation specific humidity ($g\,kg^{-1}$)	0.38	0.54
Specific humidity ($g\,kg^{-1}$)	0.38	0.59
Sensible heat flux ($W\,m^{-2}$)	5.5	8.0
Latent heat flux ($W\,m^{-2}$)	15.8	23.5
Long-wave radiation ($W\,m^{-2}$)	3.8	5.5
Short-wave radiation ($W\,m^{-2}$)	18.3	23.2

response of the thermocline (given either as the depth of the 20°C isotherm or as the maximum temperature gradient) to atmospheric forcing. Thermocline depths using either definition can typically be defined to within several meters from individual temperature profiles. The paucity of temperature profiles (Fig. 1) necessitates the use of an objective analysis routine to produce systematic portrayals of the evolution of the subsurface temperature field. REVERDIN, MOLINARI and DUPENHOAT (1985) used an objective analysis algorithm to generate monthly maps of thermocline depth field. Qualitative arguments were used to define the structure of the signal as available quantitative data were inadequate for this purpose. Similarly, the structure of the noise is defined somewhat arbitrarily. Mapping errors are dependent, in part, on data coverage, thus errors are largest near the boundaries. As a general guideline, REVERDIN, MOLINARI and DUPENHOAT (1985) considered significant anomalies are those with amplitudes twice the average mapping error, about 10 m.

3. ATMOSPHERIC OBSERVATIONS

3.1. *Surface winds*

There are two distinctly different winds regimes in the tropical Atlantic. Throughout the year, east of about 20°W the winds are predominently meridional, resembling a monsoonal-type circulation (Fig. 2). West of 20°W, the winds are predominantly zonal. The Southeast Trades are located south and the Northeast Trades north of the ITCZ. (We choose to define the position of the ITCZ as coincident with the band of minimum resultant wind speed, recognizing that other definitions are possible, e.g. maximum cloudiness [SPETH and PANITZ, 1983].) At most locations in the basin, wind speed and direction are strongly dependent on the position of the ITCZ. For instance, from February to April when the ITCZ is furthest south, winds on the equator are weakest (Fig. 2). From July to October when the ITCZ is furthest north, equatorial winds are strongest.

Monthly winds evaluated from the historical data set from 1850–1979 (HARRISON, personal communication) are used to determine the "normalcy" of the 1979 wind field. Anomaly vectors indicating vector differences greater than 2 m sec^{-1} between the 1979 and climatological winds are shown in Fig. 3. North of the equator, between 20°W and 40°W, from February to May, the vectors show a stronger southerly component during 1979. By July, in this region and further south, anomaly vectors have reversed direction with an increased northerly component. In the east the trend is somewhat reversed, with anomalously higher northerly components from December to March and higher southerly components during the remainder of the year.

The ITCZ is located within out grid from December 1978 to May 1979. Mean monthly positions of the ITCZ during 1979 (when adequately defined) and from climatology (HASTENRATH and LAMB, 1977) are shown in Fig. 4. The ITCZ's from both representations are similar in shape and position. There is some suggestion that the ITCZ is located somewhat further north than "normal" from February to April. This anomaly is consistent with the increase in southerly winds shown near the equator in the central Atlantic during this period (Fig. 3).

Winds along the equator have particular relevance to equatorial dynamics and frequently are used to drive numerical models of the region. Thus, we consider the evolution of the 1979 equatorial winds relative to the climatological winds in Fig. 5. In general, the 1979 equatorial winds are quite similar to the climatological winds throughout the basin. The

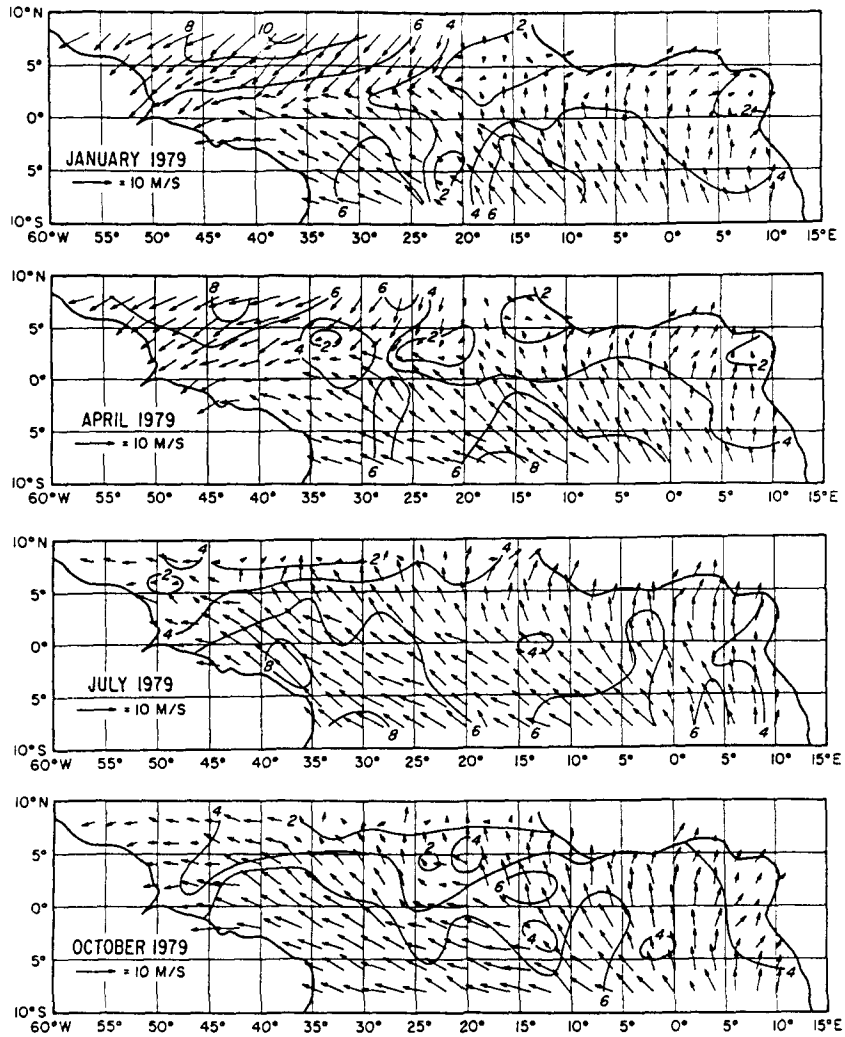

FIG. 2. Surface wind fields during 1979, from MOLINARI *et al.* (1985a).

additional structure in the 1979 wind field at 20°W as compared to the other locations is probably related to the paucity of data in this area (Fig. 1). Although the major events (e.g. February–March–April relaxation and May enhancement) occur at the same time during 1979 as in the climatology, the 1979 winds are consistently higher thoughout the basin through the summer. These positive anomalies are consistent with a more northerly position of the ITCZ during 1979 (Fig. 4).

Data distribution is such that winds can be resolved on a shorter time scale along the equator. Zonal and meridional wind components have been averaged by week onto a 2° × 2° grid along 0° and the resulting time series are shown in Fig. 6. The paucity of data in the central equatorial Atlantic is apparent in this figure. There is considerable structure in these records, much of which appears coherent in time and space, at this resolution. Of dynamical interest is the basin-wide relaxation of both components during the third week

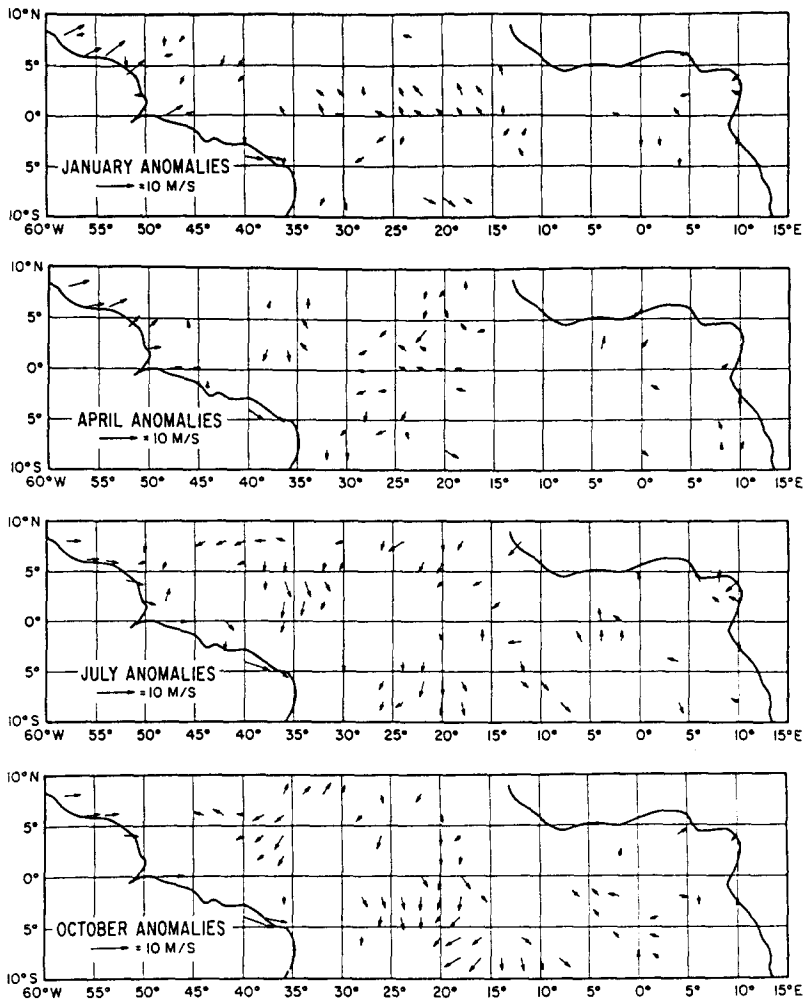

FIG. 3. Vector differences between the 1979 (from MOLINARI *et al.*, 1985a) and climatological (from HARRISON, personal communication) winds for those differences with a magnitude greater than 2 m sec^{-1}.

of April, followed by a basin-wide increase during the first week of May. This onset is associated with the northward migration of the ITCZ. During FGGE, a meteorological station was deployed near the equator at St. Peter and St. Paul Rocks (GARZOLI, KATZ, PANITZ and SPETH, 1982). Comparison of these winds with climatological winds shows that the onset of the winds during 1979 occurred during the first week of May, less than one month earlier than the historical mean. This difference would not be resolved by monthly representations of the 1979 winds (Fig. 5).

In a recent work, GARZOLI and KATZ (1983) studied the response of the NECC to seasonal wind variations. They assumed that the NECC was in geostrophic balance and analyzed the variability of the thermal structure associated with the current. They concluded that in the interior of the basin the reversal of the trade winds is responsible for the

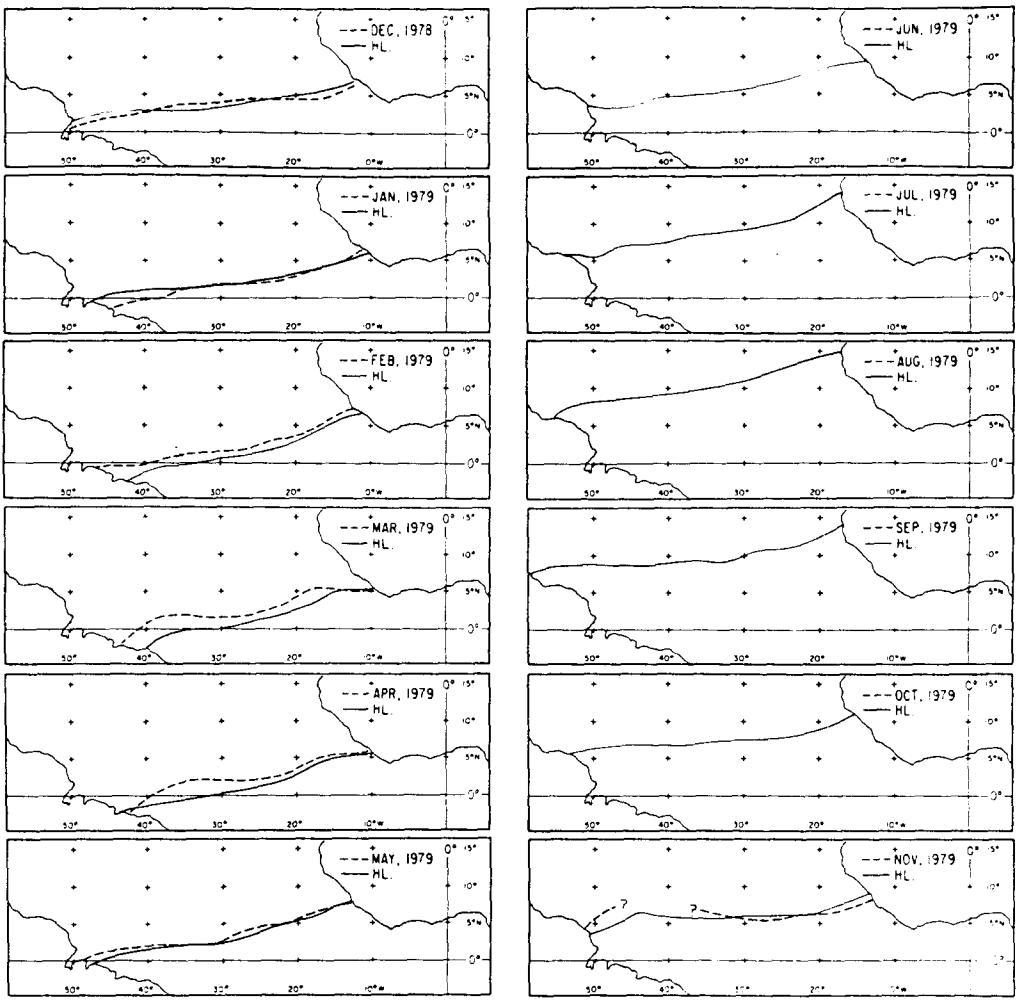

FIG. 4. The position of the ITCZ during 1979 when within the observation grid (9°S to 9°N) and from climatology (HASTERNRATH and LAMB, 1977).

reversal of the NECC through the combined mechanisms of local Ekman pumping and the divergence of the geostrophic currents. Following that work, we calculate curl $(\bar{\tau}/f)$ using the wind field just described. Our grid does not extend as far north as theirs, so we are only able to compute curls at 5° and 7°N. We impose an annual sinusoidal cycle on the time series and the resulting time-longitude plots are shown in Fig. 7 to represent the field of curl $(\bar{\tau}/f)$ on the southern and northern boundaries of the NECC. At 5°N, we also show the zero curl contour and maximum curl from the climatological representation of the curl from GARZOLI and KATZ (1983).

At 5°N, in terms of the change in sign of the curl, 1979 is quite similar to the climatology (Fig. 7). The curl changes from cyclonic to aniticyclonic in May–June in both representations. In addition, the maxima in curl occurs at the same time, during February and August. However, during 1979, the maxima appear shifted somewhat to the west.

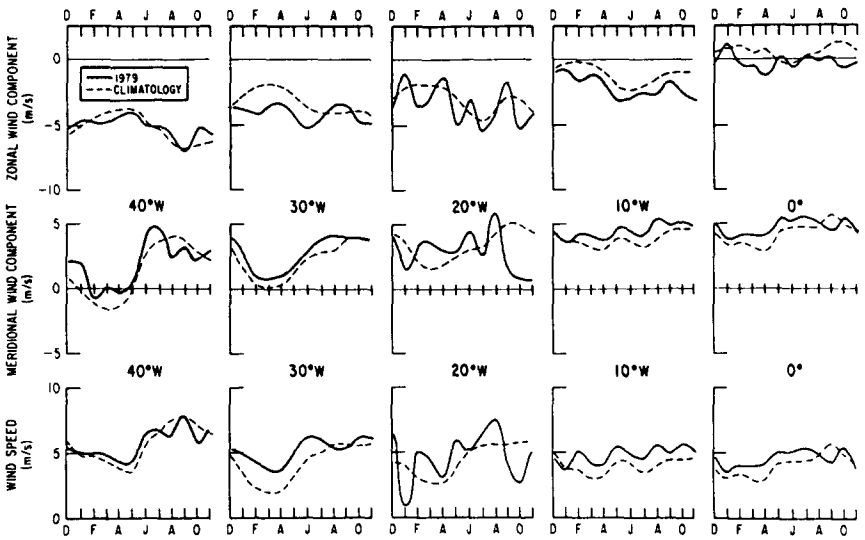

FIG. 5. Comparison of the mean-monthly wind component time series obtained during 1979 and from climatology (HARRISON, personal communication) along the equator.

GARZOLI and KATZ (1983), comparing the climatological wind curls at 5°N and 9°N, found that west of 20°W the annual variation of the curl on the southern side of the NECC fluctuates 180° out of phase with the oscillation on the northern side. In the east the curls are more in phase. Since our data permit curl calculations only at 7°N, this phase relation is not as strong. However, even though we are not at the northern boundary of the NECC there is some suggestion of the reversal in phase (Fig. 7).

3.2. *Surface heat fluxes*

The mean annual fields of latent and sensible heat flux, net shortwave radiation and net oceanic heat gain are shown in Fig. 8. Net longwave radiation is not shown, as the field is quite flat with values close to 60 $W m^{-2}$. The 1979 patterns are very similar to the climatological patterns given by HASTENRATH and LAMB (1978), also shown in Fig. 8. However, the latent heat fluxes and to a lesser degree sensible heat fluxes were greater than average during 1979. MOLINARI, FESTA and MARMOLEJO (1985a) relate these anomalies in part to the increased wind speeds observed during FGGE (Fig. 6). The increase in latent heat flux results in a decrease in net oceanic heat gain as demonstrated in Fig. 8. MOLINARI, FESTA and MARMOLEJO (1985a) note that the negative anomalies in heat gain are largest during June, July and August along the equator.

4. OCEANOGRAPHIC OBSERVATIONS

4.1. *Near surface currents*

MOLINARI, FESTA and MARMOLEJO (1985b) describe the 1979 surface current fields as derived from ship-drift reports. They averaged the raw data by month onto a 6° of latitude by 10° of longitude grid and were able to reproduce many of the features observed during

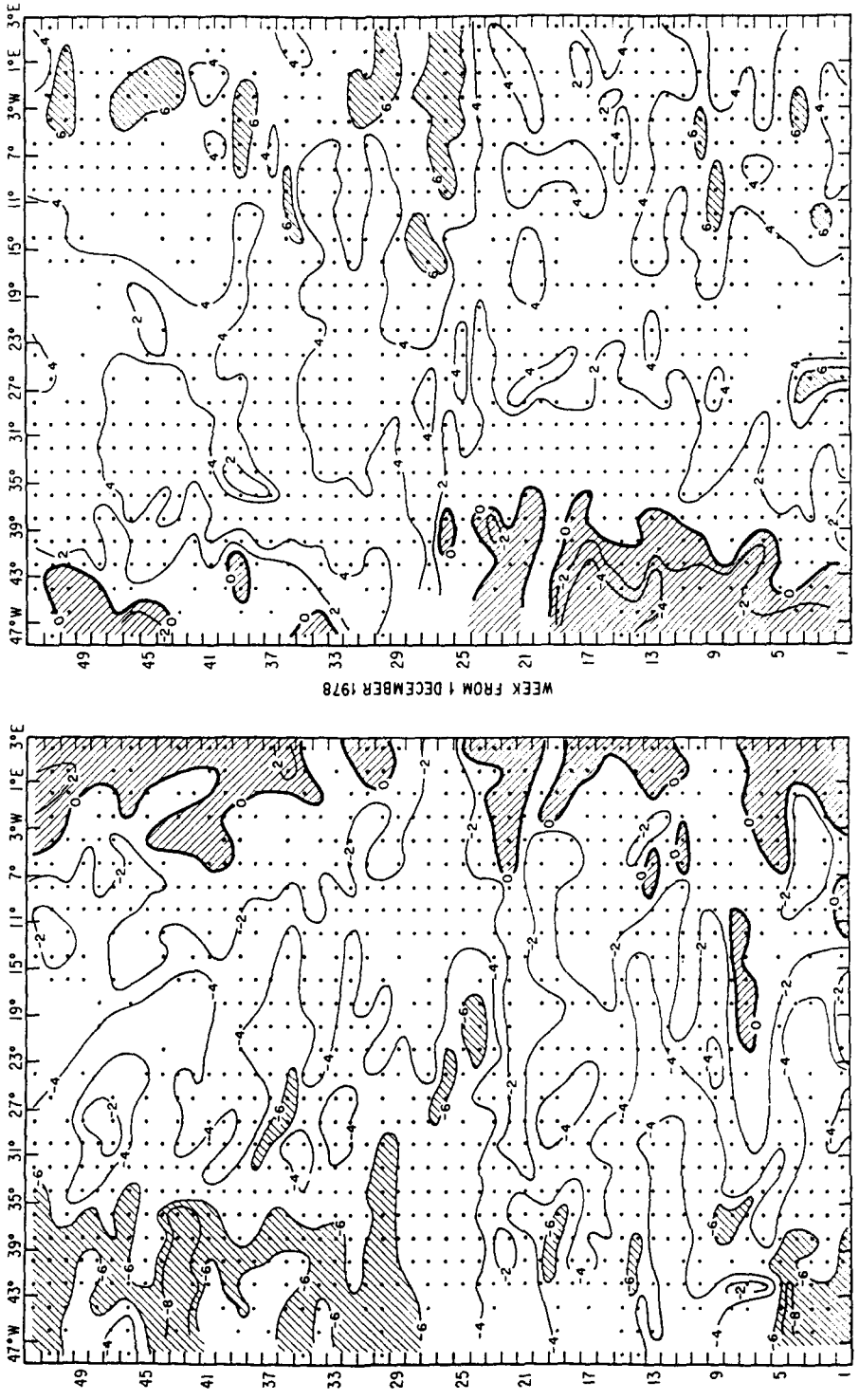

FIG. 6. Time longitude plots of the evolution of the zonal/(left panel) and meridional/(right panel) components of wind along the equator from winds averaged by week and 2° of latitude by 2° of longitude. The dots represent quadrangles with available data.

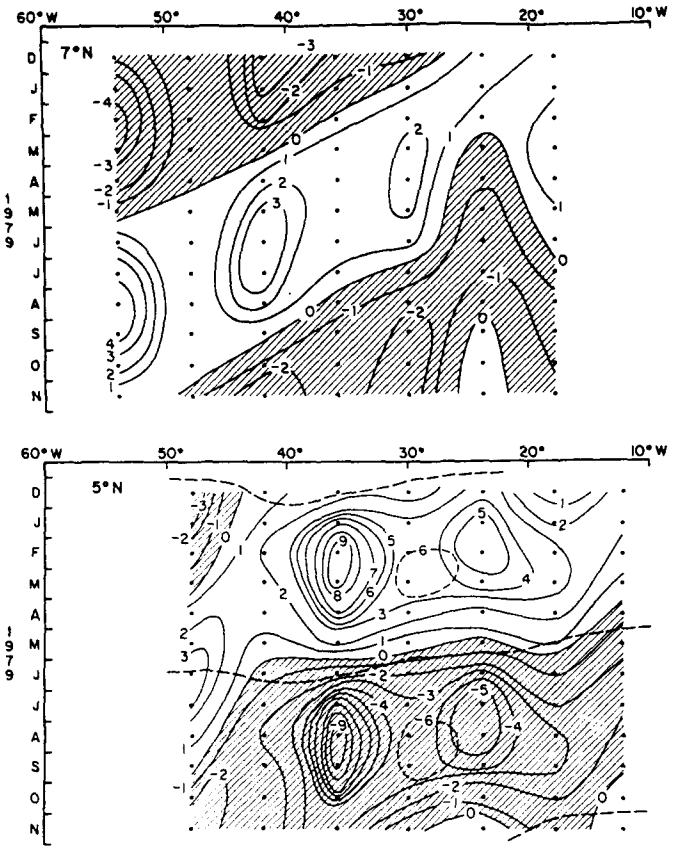

FIG. 7. Time–longitude plots of the curl ($\bar{\tau}/f$), units of dyne cm^{-3}, computed from the monthly 2° × 2° wind data of MOLINARI *et al.* (1985a) along 5°N and 7°N. The annual mean has been subtracted from each 6° of longitude average series. The zero and maximum curl contours (dashed lines) from the climatology of GARZOLI and KATZ (1983) are shown on the 5°N plot.

FGGE with direct current measurements. Along the shipping lanes (Fig. 1), better spatial resolution is possible and the zonal components of current are averaged by 3° of latitude and 5° of longitude intervals (we do not feel the observations of meridional current are significant).

Three-month running averages of the 1979 monthly ship-drift data were computed and resulting time–latitude plots along the western and eastern shipping lanes (Fig. 1) are shown in Fig. 9. In the west the South Equatorial Current (SEC) can be characterized by an annual cycle in both the position and intensity of the flow along its axis. During May the axis of the SEC is located furthest south. From July through September, an intensified SEC is observed on and north of 0°. During April eastward flow is observed near the equator and the North Equatorial Countercurrent (NECC) does not appear at these longitudes. From June through October, the NECC appears in the western basin. Thus, the intensities of the NECC and SEC are in phase. In the east, the eastern extension of the NECC, the Guinea Current, flows throughout the year, with no annual signal discernible from these data. The SEC is strongest near the equator from June through October, with eastward flow observed here south of 0° from January through March. Direct observations of eastward equatorial flow at 22°W are described by FAHRBACH (1983).

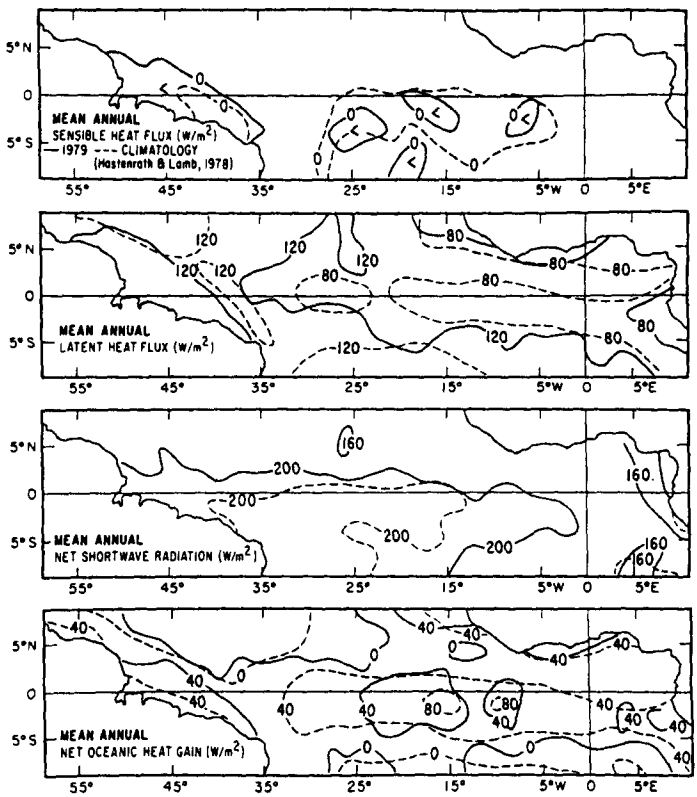

FIG. 8. Mean annual distributions of net long- and short-wave radiation, latent heat flux and net oceanic heat gain, all in $W m^{-2}$, computed from data given in MOLINARI *et al.* (1985a).

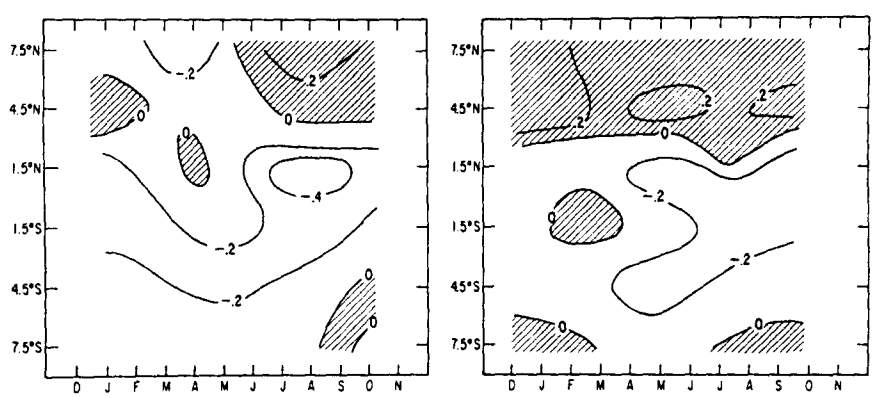

FIG. 9. Time–latitude plots of zonal surface current speed ($m sec^{-1}$) derived from ship-drift data obtained along the western and eastern shipping lanes (Fig. 1) and averaged onto a monthly 3° × 5° grid.

The FGGE ship-drift data are compared to the climatological data of RICHARDSON and MCKEE (1984) in Fig. 10. At and north of 1.5°S in the west, FGGE was in general a "normal year" in terms of both the amplitude (within about 0.1 $m sec^{-1}$) and phase (within one month) of the SEC and NECC. South of 1.5°S, the SEC was typically somewhat weaker

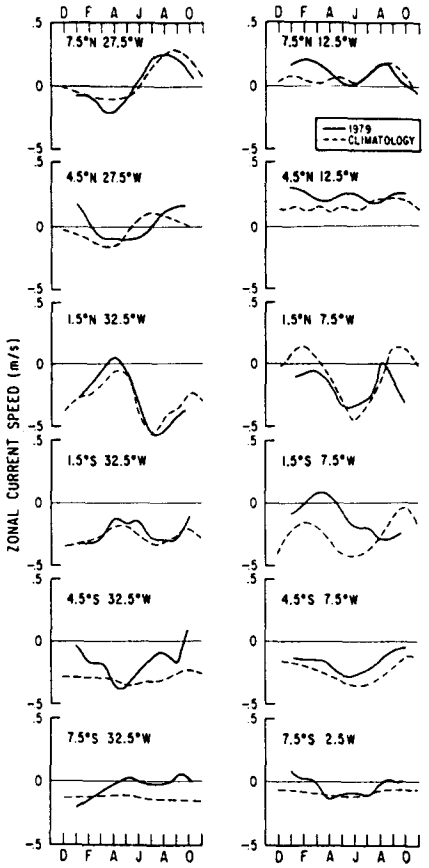

FIG. 10. Comparison of zonal current components (m sec^{-1}) obtained from ship-drift data during 1979 and climatological averages (from RICHARDSON and MCKEE, 1984).

during FGGE. Similarly, along the eastern shipping lane, flows at and north of 1.5°N are "normal." The SEC was somewhat weaker in the south. The apparently abnormal time series at 1.5°S can be explained by a southward shift in the extent of the eastward flowing Guinea Current. Thus, in both the western and eastern Atlantic, there is a reduction in the westward component of the flow on and south of the equator throughout most of the year. This result is probably real and not an artifact of the ship-drift data, as the zonal winds in these regions were anomalously westward (Fig. 6).

Prior to FGGE, data were inadequate to consider the annual cycle of the Equatorial Undercurrent. Data collected during FGGE span the year, albeit in an uneven fashion. KATZ, MOLINARI, CARTWRIGHT, HISARD, LASS and DE MESQUITA (1981) reported on data from 28 profiling sections and found an annual mean of 21 $\times$ 10^6 m^3 sec^{-1}, relative to 500 m, with a range from 10 to 44 $\times$ 10^6 m^3 sec^{-1} in the central basin (25° to 33°W). Of the 23 values in the central basin, the three largest transports occurred between the last week in January and the first week in March. The average transport was 35 $\times$ 10^6 m^3 sec^{-1}. The three lowest values were obtained between the last week in May and the middle of July and average 12 $\times$ 10^6 m^3 sec^{-1}.

Data somewhat to the east were reported by BUBNOV (1982) from current meter arrays. Two sites were occupied for two periods: 18.5°W and 23.5°W and March/April and

July/August. Data from the western location show a reverse trend from the above: increased transport during July/August. The difference between the mooring and profiling measurements in the spring derives from the fact that large values of transport reported by KATZ *et al.* (1981) occur only when the surface layer is also flowing eastward. We know from ship-drift observations that this is more likely to occur in the western than eastern Altantic, although some eastward flow is also observed at 7.5°W during January, February and March 1979 (Fig. 9). To complicate the situation, BUBNOV (March 1983 issue of *Tropical Ocean-Atmosphere Newsletter*, unpublished document) reported no surface eastward flow at 23.5°W during the period of his 1979 observations. These results suggest that "surfacing of the undercurrent" varies temporally and spatially, with the surface layers possibly responding on a short time scale (few days) to local wind conditions.

Observations of the South Equatorial Undercurrent (SEUC) were also obtained during FGGE (MOLINARI, VOITURIEZ and DUNCAN, 1981). This subsurface eastward flow is typically observed between 3°S and 5°S, with maximum speeds at 150 m. The SEUC was crossed on two July/August and two February/March cruises in the period extending from August 1978 to March 1980. These and historical SEUC data are inadequate to discern any seasonal variability in the intensity of the SEUC (MOLINARI, VOITURIEZ and DUNCAN, 1981). A similar Undercurrent has been observed north of the equator (COCHRANE, KELLY and OLLING, 1979), but few sections were taken during FGGE in this region.

4.2. *Thermocline depth*

The tropical thermocline depth (defined either as the depth of the 20°C isotherm or maximum vertical temperature gradient) distribution is frequently used as an inverse surrogate for the surface pressure field. We will adopt this assumption. REVERDIN, MOLINARI and DUPENHOAT (1985) generated monthly 20°C isothermal depth distributions from January to August 1979 using an objective analysis algorithm. In general, the distributions can be characterized as a series of zonally oriented ridges and troughs superimposed on an east–west slope (Fig. 11). The thermocline depth anomalies observed during FGGE perturbed climatological features but caused no qualitative differences from the climatology. In the central Atlantic (10°W to 40°W), a ridge in the thermocline is centered at about 3°S, during January, February, and March (note: a ridge [trough] in thermocline topography is equivalent to a trough [ridge] in sea-surface topography). Proceeding north during the same months, a thermocline trough is observed on the equator, a ridge at about 2°N and another trough at 5°N. In April the thermocline at 5°N begins to rise and the thermocline at 2°N begins to fall. By July, the pattern described by KATZ (1981) is observed (e.g. an equatorial ridge bounded on the north by a countercurrent trough). Data are not available to describe the evolution of the thermocline after August 1979. However, climatological distributions (MERLE and DELCROIX, 1985) indicate that the August pattern would persist through October in a "normal" year. The thermocline would then begin to evolve to the January pattern in November and December.

Increased data coverage along the equator also permits us to consider in somewhat more detail the east–west thermocline slope along 0°. First, we consider the historical data-set (as used in MERLE and DELCROIX, 1985), using the depth of maximum vertical gradient to define the thermocline position. Gaps in the time-series are filled by fitting a sinusoidal curve of annual period to the data. The result is shown in Fig. 12. The fit differs from the data with a standard deviation of 11 m. The evolution of this field can be

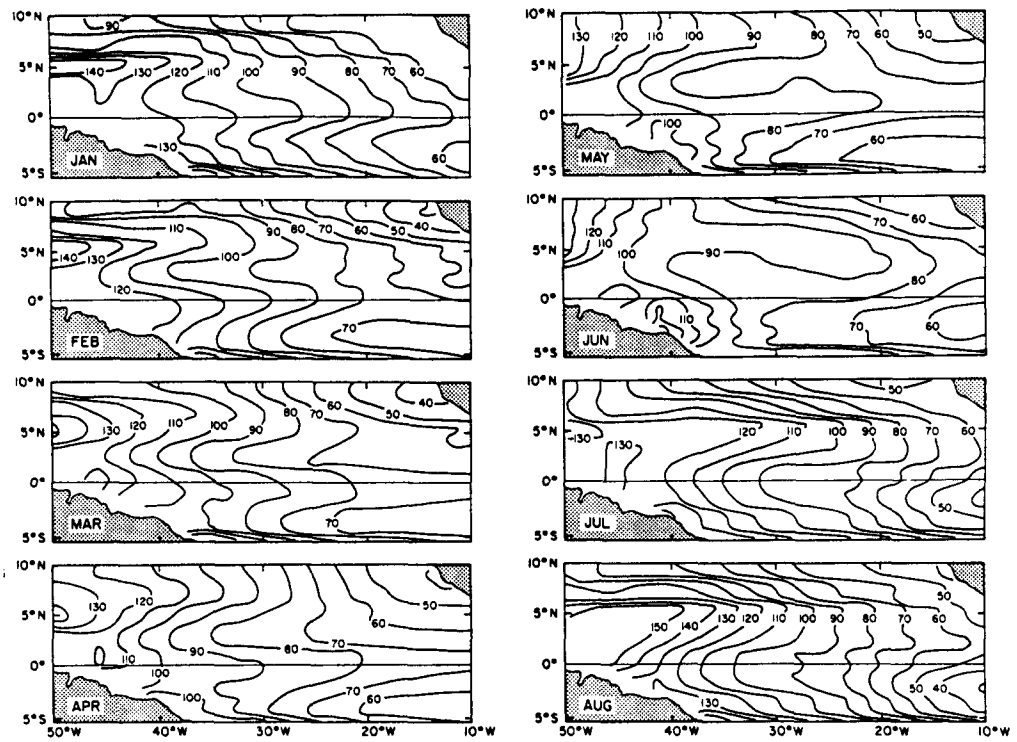

FIG. 11. Thermocline depth (m) fields given as the depth of the 20°C isotherm and derived from an objective analysis algorithm from REVERDIN *et al.* (1985).

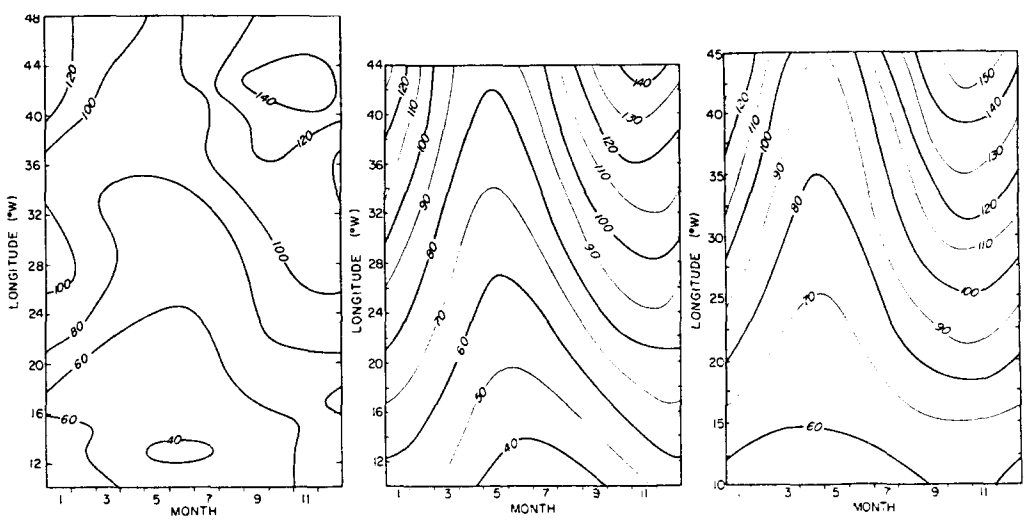

FIG. 12. Left panel: Thermocline depth distribution, in m, determined from the climatological data set of MERLE and DELCROIX (1985). Missing values have been supplied by fitting a sinusoidal curve of annual period to the data. Center panel: Representing the thermocline distribution in the left panel by equation (1), i.e. the sum of an average annual slope, a basin-wide sinusoidal vertical motion about that linear slope and a rotation of the thermocline about a central pivot point. Right panel: The thermocline depth distribution determined by fitting equation (2) in a least squares sense, to the 1979 data.

represented by a sum of three terms: an annual average linear slope, a basin-wide sinusoidal vertical motion about that linear slope and a rotation of the thermocline (in a zonal plane) about a central pivot point. Mathematically, the depth D of any point on the equator between 10°W and 44°W is given by

$$D(x, t) = 78.4 + 2.015(x - x_0) + 18.24\cos(\pi N/6 + 0.400) + 0.822(x - x_0)\cos(\pi N/6 + 1.031) \quad (1)$$

where $x_0 = 27.1$°W and N is the number of months. This function is also plotted in Fig. 12 and it differs from the first representation with a standard deviation of 7 m.

If we assume that the form of the thermocline as given above is correct for any specific year, then we ask what the mean depth and slope of the thermocline and the amplitude and phase of the two vertical motions were during 1979. That is, we fit the FGGE-year data with

$$D(x, t) = A + B(x - x_0) + C\cos(\pi N/6 + 0.400 + \phi_1) + D(x - x_0)\cos(\pi N/6 + 1.031 + \phi_2) \quad (2)$$

where A, B, C and D and ϕ_1 and ϕ_2 represent the unknown amplitudes and phases, respectively, which are determined in a least squares sense. The resulting thermocline distribution is shown in Fig. 12. A comparison of the climatological and 1979 parameters are given in Table 4. The equatorial thermocline is some 10 m deeper during FGGE, consistent with the findings of REVERDIN, MOLINARI and DUPENHOAT (1985). The mean annual slope and amplitude of the up/down motion are similar, but the amplitude of the seesaw motion is greater during FGGE. The phases of the two motions are somewhat different, with the up/down motion occurring earlier and the seesaw motion occurring later during FGGE.

As before, if we assume that NECC is in geostroophic balance, then we can use the thermal structure in the region to study its annual variability. The depth of the thermocline is defined as the depth of the maximum gradient in the temperature profile. Due to the lack of data, distributions of this parameter are computed by averaging data in 5° × 2° boxes at every degree of latitude and at every 2° in longitude. The values are smoothed, interpolated and extrapolated by imposing an annual sinusoidal cycle. If the NECC is in geostrophic balance, then changes in the meridional slope indicate changes in zonal velocity and transport.

TABLE 4. COMPARISON OF 1979 AND CLIMATOLOGICAL PROPERTIES OF EQUATORIAL THERMOCLINE MOVEMENTS AS GIVEN BY EQUATION (2)

Parameter	Units	Historical	FGGE
1. Mean annual depth at 27.5°W (A)	m	78.4	88.7
2. Mean annual slope (B)	m/°long	2.01	1.96
3. Amplitude of annual up/down motion (C)	m	18.2	17.6
4. Phase of annual up/down motion (ϕ_1)	days from 15 Dec.	−23	−49
5. Amplitude of annual seesaw motion (D)	m/°long	0.82	1.00
6. Phase of annual seesaw motion (ϕ_2)	days from 15 Dec.	−60	−46
7. Percent variance explained by sinusoidal fit	%	93	85

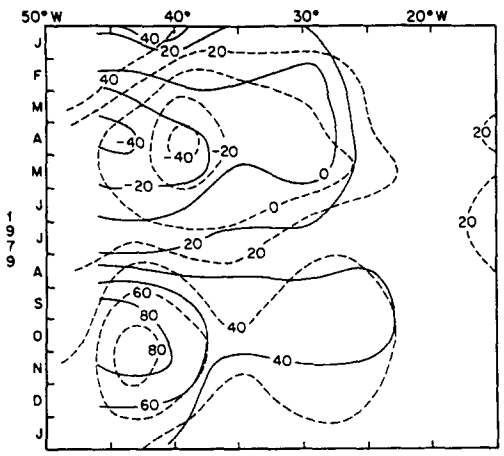

FIG. 13. Meridional difference (3°N–9°N) of the thermocline depth, in m, across the NECC as a function of month and longitude computed from the climatological data of GARZOLI and KATZ (1983), dashed lines and 1979 data, solid lines.

Figure 13 shows the meridional difference of the thermocline depth across the NECC between 4° and 9°N as a function of time and longitude derived from the 1979 observations and the climatology of GARZOLI and KATZ (1983). The 1979 onset, location and amplitude of the NECC agree quite well with climatology (as to be expected from Fig. 9). The main difference is a westward shift by about 5° of the centre of the westward flow in 1979, a shift also noted in the curl distribution at 5°N (Fig. 8).

4.3. *Sea-surface temperature*

Mean monthly distributions of SST from MOLINARI, FESTA and MARMOLEJO (1985a) are shown in Fig. 14. The annual cycle of the large-scale SST pattern is very similar to the cycle derived from climatological data sets as given by HASTENRATH and LAMB (1977), for instance. In particular, highest temperatures and smallest horizontal temperature gradients occur during March and April. Lowest temperatures appear during July, August and September in a cold water tongue which extends from the eastern to the central basin and is positioned asymmetrically about the equator. Largest horizontal temperature gradients in both the meridional and zonal directions occur at this time.

Monthly SST anomaly plots (referred to the smoothed climatology of Reynolds, 1983) representative of the four seasons are given in Fig. 15. In general, anomalies of the same sign are oriented in north–south bands and extend from the southern boundary of the grid (9°S or South America) to the northern boundary (9°N or Africa). For example, during January and April, from 35°W to the western boundary and from 10°W to 20°W the anomalies are predominantly cold, while from 20°W and 35°W and from the eastern boundary to 10°W, the anomalies are predominantly warm (Fig. 15). The region of negative anomalies between 10°W and 20°W decreases in size during April and by July warm anomalies extend from 0° to 35°W, with predominantly cold anomalies located near the boundaries. In November (not shown) the region of negative anomalies reappears around 15°W. Thus, over most of the central Atlantic from 9°S to 9°N and from May to October, SST's were anomalously high (of the order 1°C).

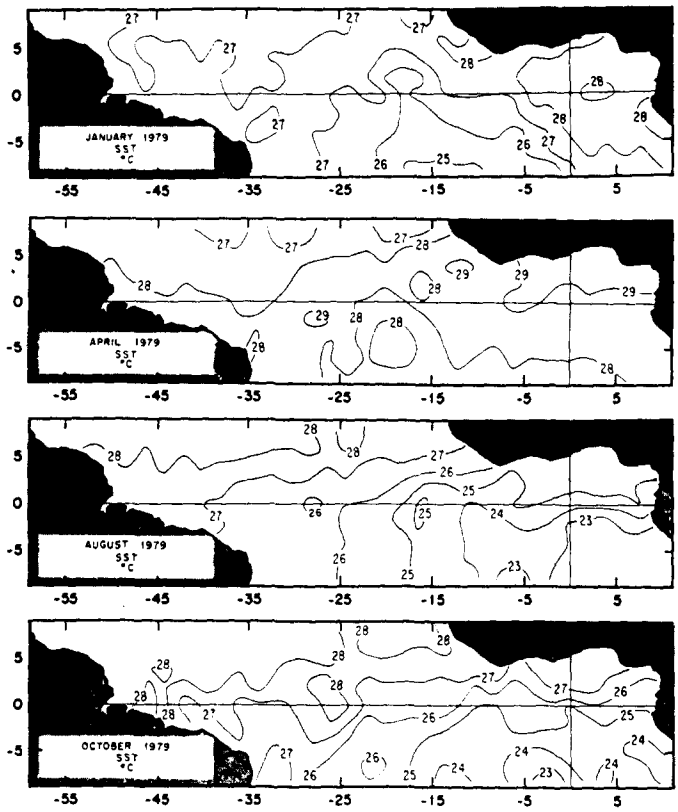

FIG. 14. Sea surface temperature fields (°C) observed during 1979 (from MOLINARI *et al.*, 1985a).

Time series of equatorial SST's are shown in Fig. 16. The 1979 May, June, July cooling which leads to the formation of the cold water tongue (Fig. 15) is in phase with the onset of the climatological cooling. However, between 10°W and 30°W the cooling is not as intense during FGGE.

5. DISCUSSION

We recognize that some form of numerical or inverse model is required to take full advantage of the FGGE data. These models would be forced at the surface with the FGGE winds and heat fluxes and would use the subsurface oceanographic data for consistency checks, initial conditions and/or input to update the model. Numerical models using the FGGE surface boundary conditions are planned (G. PHILANDER, personal communication). We therefore confine our remarks to a general discussion of the oceanic response to the seasonally varying surface wind field.

Surface current, thermocline depth and SST variability along the equator have been attributed to surface wind forcing. If the winds during 1979 vary as predicted by climatology, we expect that these oceanic events will also occur as predicted by climatology (to within the resolution of the data). Our expectations are realized comparing the FGGE and climatological time series.

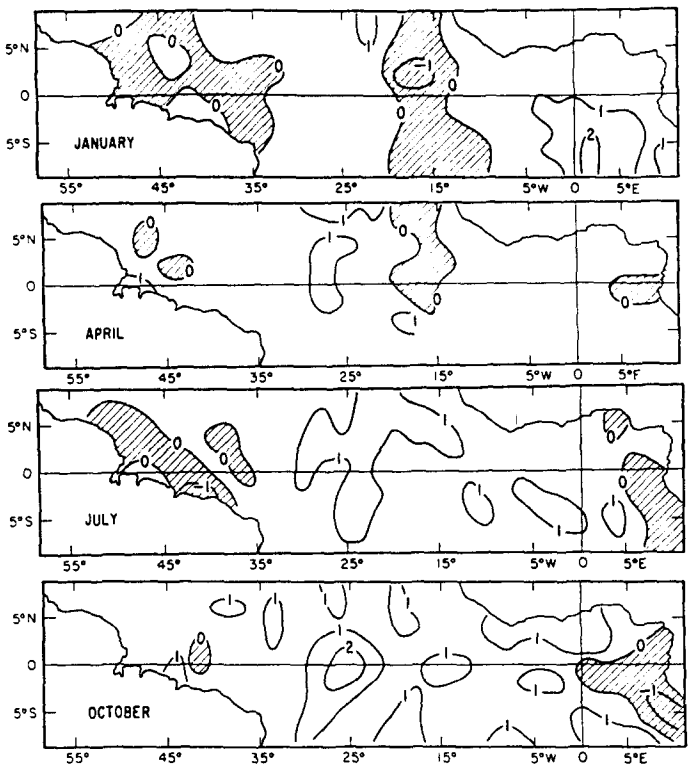

FIG. 15. Differences (°C) between the SST climatology REYNOLDS (1983) and the 1979 SST fields.

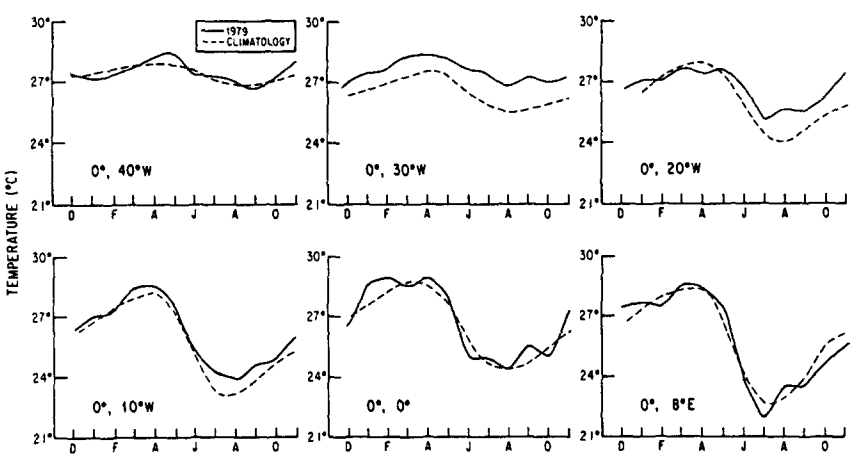

FIG. 16. Climatological (REYNOLDS, 1983) and 1979 SST time series along the equator.

Thermocline depth changes along the equator and the associate changes in equatorial pressure have been modelled as the ocean's response to either sudden or periodic onsets and relaxations of the zonal winds (O'BRIEN, ADAMEC and MOORE, 1978; PHILANDER, 1981; CANE and SARACHIK, 1981, for instance). The initial response to wind changes is in the form

of propagating Kelvin and Rossby waves. Steady or quasi-steady state thermocline depth distributions are established in the wake of these waves. The FGGE data presented herein are inadequate to resolve the various waves. The resulting thermocline adjustments do occur within one month of climatology (Table 4) as to be expected in view of the timing of the 1979 onset relative to the climatological onset (Fig. 5).

Surfacing of and increased eastward transport by the EUC is also predicted in models when the zonal winds relax (CANE, 1980). As first noted by KATZ *et al.* (1981), these features are observed during FGGE in February, March, April consistent with the wind relaxation at this time.

Equatorial unwelling and the cold water tongue have been attributed to onsets of both the zonal wind component through thermocline adjustments [PHILANDER and PACANOWSKI (1980), for instance] and meridional wind components through thermocline adjustments and horizontal advection [PHILANDER and PACANOWSKI (1981), for instance]. Onsets of either wind component can also cause an acceleration of the SEC. The equatorial unwelling, cold water tongue and SEC acceleration during FGGE all occur at the time predicted by climatology (Fig. 16 and Fig. 10) as expected in view of the associated wind onset (Fig. 5). The higher SST's and reduced SEC speeds near 0° may be related to the reduction in the southerly component of the Southeast Trades during July (Fig. 3). The results of the PHILANDER and PACANOWSKI (1981) model suggest such a response.

Finally, the onset and the disappearance of the NECC in the western Atlantic are in phase with the changes in the distribution of wind stress curl as first predicted from climatology by GARZOLI and KATZ (1983). Not only are the FGGE and climatological events in phase, but both the position of the maximum curl and the maximum thermocline gradient are located further to the west during FGGE.

There are some oceanic anomalies not readily explainable in terms of atmospheric anomalies, but which nevertheless are explainable in terms of oceanic processes. For instance, from June through November mid-basin equatorial SST's are anomalously high (Fig. 16), although surface heat fluxes are anomalously low (MOLINARI, FESTA and MARMOLEJO, 1985a). However, during 1979, the equatorial thermocline is some 10 m deeper than normal (Table 4) and there is a reduction in the westward component of surface flow on and south of the equator (Fig. 9) compared to climatology [both features reminiscent of El Niño conditions in the Pacific (CANE, 1983)]. A deeper thermocline implies increased upwelling is required to lower SST to shallower thermocline values. Decreased westward flow implies reduced effects of advection on surface cooling (PHILANDER and PACANOWSKI, 1981). The deeper thermocline which occurs throughout the period of available data is not easily related to anomalies in the surface forcing fields.

In summary, the response of the upper ocean during 1979 to the annual cycle of surface winds is consistent with the timing of major atmospheric events. There are some differences between the amplitudes of FGGE and climatological events which will require models to resolve. These results are encouraging in that they were derived from ship-of-opportunity and essentially uncoordinated research vessel efforts and suggest that results from the recently completed FOCAL/SEQUAL programs (ANON, 1984) and the planned TOGA effort should further define the oceanic response since these efforts were/will be coordinated. The FGGE results further indicate that ship-of-opportunity data routinely collected by merchant ships can make a valuable contribution to studies of the tropical oceans. Thus, concentrated efforts should be made to ensure that these data are incorporated into future work in these areas.

Acknowledgements—R. L. M. was partially supported by the NOAA Special Research Projects Office; S. G. and E. K. by NSF Grant ATM-8109197; D. E. H. by NASA Grant NAG5-322, NSF Grant OCE 83-01787 and the NOAA Pacific Marine Environmental Laboratory and EPOCS and TOGA Programs.

REFERENCES

ANON (1982) SEQUAL: A study of the equatorial Atlantic Ocean. *EOS, Transactions AGU, 14.*

BUBNOV, V. A. (1982) On seasonal variability of the Lomonosov Current. *Oceanology*, **22**, 26–29.

BUNKER, A. F. (1976) Computations of surface energy flux and annual air–sea interaction cycles of the North Atlantic Ocean. *Monthly Weather Reviews*, **104**, 1122–1140.

CANE, M. (1980) On the dynamics of equatorial currents, with applications to the Indian Ocean. *Deep-Sea Research*, **27**, 525–544.

CANE, M. (1984) Oceanographic events during El Niño. *Science*, **222**, 1189–1195.

CANE, M. and E. SARACHIK (1981) The response of a linear baroclinic equatorial ocean to periodic forcing. *Journal of Marine Research*, **39**, 651–693.

COCHRANE, J. D., F. J. KELLY and C. R. OLLING (1979) Subthermocline countercurrents in the western equatorial Atlantic Ocean. *Journal of Physical Oceanography*, **9**, 724–738.

FAHRBACH, E. (1983) On the variation of the heat content in various vertical layers in the central Atlantic Ocean during FGGE. *In: Hydrodynamics of the equatorial ocean*, J. C. J. NIHOUL, editor, Elsevier Science Publishers, Amsterdam, 83–98.

FAHRBACH, E. and E. BAUERFIEND (1982) The variability of equatorial thermocline spreading as an indicator of equatorial upwelling in the Altantic Ocean. *Oceanography of the Tropics*, **2**, 121–132.

GARZOLI, S. L. and E. J. KATZ (1983) The forced annual reversal of the Atlantic North Equatorial Countercurrent. *Journal of Physical Oceanography*, **13**, 2082–2090.

GARZOLI, S. L., E. J. KATZ, H. J. PANITZ and P. SPETH (1982) *In-situ* wind measurements in the equatorial Atlantic during 1979. *Oceanologica Acta*, **5**, 281–288.

HASTENRATH, S. and P. LAMB (1977) *Climatic atlas of the tropical Atlantic and eastern Pacific oceans.* University of Wisconsin Press.

HASTENRATH, S. and P. LAMB (1978) *Heat budget atlas of the tropical Atlantic and eastern Pacific oceans.* University of Wisconsin Press.

KATZ, E. J. (1981). Dynamic topography of the sea surface in the equatorial Atlantic. *Journal of Marine Research*, **39**, 53–63.

KATZ, E. J. and S. L. GARZOLI (1981) Response of the western equatorial Atlantic Ocean to an annual wind cycle. *Journal of Marine Research*, **40** (suppl.), 307–327.

KATZ, E. J., R. L. MOLINARI, D. E. CARTWRIGHT, P. HISARD, H. U. LASS and A. DE MESQUITA (1981) The seasonal transport of the Equatorial Undercurrent in the western Atlantic (during the Global Weather Experiment). *Oceanologica Acta*, **4**, 445–450.

LASS, H. U., U. BUBNOV, J. M. HUTHNANCE, E. J. KATZ, J. MEINCKE, A. DE MESQUITA, F. OSTAPOFF and B. VOITURIEZ (1983) Seasonal changes of the zonal pressure gradient in the equatorial Atlantic during the FGGE year. *Oceanologica Acta*, **6**, 3–11.

MCCREARY, J. P., D. W. MOORE and J. M. WITTE (1981) *A Report of the Final Meeting of SCOR Working Group 47 in Venice, Italy.* Nova University Press/N.Y.I.T. Press, Fort Lauderdale, Florida, 466 pp.

MERLE, J. (1978) Atlas Hydrologique Saisonnier de l'Ocean Atlantique Intertropical. *Travaux et Documents de l'O.R.S.T.O.M.*, No. 82, 184 pp.

MERLE, J. and T. DELCROIX (1985) Seasonal variability in the thermocline depth in the tropical Atlantic Ocean. *Journal of Physical Oceanography*, in press.

MERLE, J., M. FIEUX and P. HISARD (1980) Annual signal and interannual anomalies of sea surface temperature in the eastern equatorial Atlantic Ocean. In: *Equatorial and A-Scale Oceanography*, Supp. II to *Deep-Sea Research*, **26A**, 77–101.

MEYER, S. L. (1975) *Data-analyses for scientists and engineers.* John Wiley Inc., NY, 513 pp.

MOLINARI, R. L. (1982) Observations of eastward currents in the tropical South Atlantic Ocean (1978–1980). *Journal of Geophysical Research*, **87**, 9707–9714.

MOLINARI, R. L. (1983) Satellite-tracked drifting buoy observations of near-surface currents and temperature in the central and western tropical Atlantic. *Journal of Geophysical Research*, **88**, 4433–4438.

MOLINARI, R. L., B. VOITURIEZ and P. DUNCAN (1981) Observations in the subthermocline undercurrent of the Equatorial South Atlantic Ocean: 1978–1980. *Oceanologica Acta*, **4**, 451–456.

MOLINARI, R. L., E. KATZ, E. FAHRBACH, H. U. LASS and B. VOITURIEZ (1983). Near surface temperature observations obtained in the equatorial Atlantic Ocean during FGGE (1979). In: *Hydrodynamics of the equatorial ocean*, J. C. J. NIHOUL, editor, Elsevier Science Publishers, Amsterdam, 65–82.

MOLINARI, R. L., J. F. FESTA and E. MARMOLEJO (1985a). Evolution of sea-surface temperature and surface meteorological fields in the tropical Atlantic Ocean during FGGE, 1979: I. Description of surface fields and computation of surface energy fluxes. *Progress in Oceanography*, **14**, 401–420.

MOLINARI, R. L., J. F. FESTA and E. MARMOLEJO (1985b) Evolution of sea-surface temperature in the tropical Atlantic Ocean during FGGE, 1979: II. Oceanographic fields and heat balance of the mixed layer. *Journal of Marine Research*, **43**, 67–81.

O'BRIEN, J. J., D. ADAMEC and D. MOORE (1978). A simple model of equatorial upwelling in the Gulf of Guinea. *Geophysical Research Letters*, **5**, 633–636.

PHILANDER, S. G. H. (1981) The response of equatorial currents to a relaxation of the trade winds. *Journal of Physical Oceangraphy*, **11**, 176–189.

PHILANDER, S. G. H. and R. C. PACANOWSKI (1980) The generation of equatorial currents. *Journal of Geophysical Research*, **85**, 1123–1136.

PHILANDER, S. G. H. and R. C. PACANOWSKI (1981) The oceanic response to cross-equatorial winds (with application to coastal upwelling in low latitudes). *Tellus*, **33**, 201–210.

REVERDIN, G., R. L. MOLINARI and Y. DUPENHOAT (1985) Objective analysis of thermocline depth distributions obtained in the tropical Atlantic Ocean during FGGE, 1979. *Deep-Sea Research*, **33**(1), 43–53.

REYNOLDS, R. W. (1983) A comparison of sea surface temperature climatologies. *Journal of Climate and Applied Meteorology*, **22**, 447–459.

RICHARDSON, P. L. and T. K. MCKEE (1984) Average seasonal variation of the Atlantic Equatorial Currents from historical ship drift. *Journal of Physical Oceanography*, **14**, 1226–1238.

SPETH, P. and H. J. PANITZ (1983) The variability of local winds at 22°W and their influence on the oceanic system at the equator in the Atlantic during FGGE. In: *Hydrodynamics of the Equatorial Ocean*, J. C. J. Nihoul, editor, Elsevier Science Publishers, Amsterdam, 51–64.